

Controlling the heat dissipation in temperature-matched plasmonic nanostructures

Alessandro Alabastri,^{*,†} Mario Malerba,^{‡,&} Eugenio Calandrini,^{‡,&} Alejandro Manjavacas,[⊥]

Francesco De Angelis,[‡] Andrea Toma,[‡] and Remo Proietti Zaccaria^{*,#,‡}

[†]Department of Physics and Astronomy and Department of Electrical and Computer Engineering, Rice University, 6100 Main Street, Houston, Texas 77005, United States

[‡]Istituto Italiano di Tecnologia, via Morego 30, 16163 Genova, Italy

[⊥]Department of Physics and Astronomy, University of New Mexico, Albuquerque, New Mexico 87131, United States

[#]Cixi Institute of Biomedical Engineering, Ningbo Institute of Materials Technology and Engineering, Chinese Academy of Sciences, Ningbo 315201, China

[&]These authors contributed equally to this work.

*Corresponding authors: Alessandro.Alabastri@rice.edu; Remo.Proietti@iit.it

Supporting Information

Comparison between classical and plasmonic matching

In classical antenna theory, when a terminating impedance (Z_T) is applied to a receiving antenna (e.g. a dipole antenna) the current flowing through the equivalent circuit is¹:

$$I = \frac{V}{Z_T + Z_A} \quad (1)$$

where V and Z_A are the voltage and impedance of the equivalent Thévenin generator describing the antenna. We can expand the impedances into their real (resistance, R) and imaginary (reactance, X) parts as $Z_T = R_T + jX_T$ and $Z_A = R_A + jX_A$. Here R_A accounts from all the power losses from the antenna system and can be thus further decomposed into radiation resistance R_s (related to the reradiated power from the antenna) and loss resistance R_L (related to the actual dissipation into heat in the antenna). The *matching* condition refers to the case when the power (P_T) absorbed by the terminating load (R_T) is maximized. This power can be written as:

$$P_T = \frac{V^2 R_T}{(R_s + R_L + R_T)^2 + (X_A + X_T)^2} \quad (2)$$

and it is maximized (antenna *matched*) when the resistances are *matched*, $R_T = R_s + R_L$ and the reactances cancel out, $X_T = -X_A$. While the latter condition sets the system antenna/terminating impedance in resonance, the former is what constitutes the *matching* between antenna and terminal resistances allowing for the transferring of the maximum possible amount of power from the antenna to the load (R_T). Generally, both X_T and R_T belong to a transmission line and they can be tuned to reach the *matching* condition.

In the case of plasmonic nanoantennas investigated in this work, the idea is to reach the *matching* condition without introducing any external terminating impedance ($Z_T = 0$). In particular, by exploiting both the fundamental plasmon resonance and the temperature dependence damping factor one can reach the *temperature-matched* condition within the nanoantennas itself. In fact by targeting heat maximization within the nanoantenna, one can modify Eq. (2) as:

$$P_L = \frac{V^2 R_L(T)}{(R_s + R_L(T))^2 + (X_A)^2} \quad (3)$$

where $R_L(T)$ is the antenna resistance that includes the temperature effect given by $\Gamma_{e-ph}(T)$ and X_A represents the reactance of the antenna which is embedded in a background medium (vacuum, air etc.). Furthermore, by modelling the nanoantenna as a nanocircuit,²⁻⁴ at the plasmonic resonance $\omega_0 = 1/\sqrt{LC}$, the quantity $X_A = 1/\omega C - \omega L = 0$ which indeed minimizes the total reactance. Finally, the second requirement which needs to be fulfilled in order to reach the *matching* condition is all about the resistances. In this work we show that, by modifying the temperature, it is possible to achieve $R_s = R_L(T)$ thus allowing maximum dissipation into the *temperature-matched* nanoantenna.

Derivative of absorption and scattering efficiencies with respect to absorption damping

At resonance the derivatives are:

$$\begin{aligned} \frac{\partial \sigma_a}{\partial \Gamma_a} &= \frac{1}{\sigma_g} \left(\frac{N m_e e^2}{c \epsilon_0} \right) \frac{N \Gamma_s \omega_0^2 - m_e \Gamma_a}{(N \Gamma_s \omega_0^2 + m_e \Gamma_a)^3} \\ \frac{\partial \sigma_s}{\partial \Gamma_a} &= \frac{1}{\sigma_g} \left(\frac{2 N^2 m_e e^2}{c \epsilon_0} \right) \frac{\Gamma_s \omega_0^2}{(N \Gamma_s \omega_0^2 + m_e \Gamma_a)^3} \end{aligned} \quad (4)$$

Electron-phonon scattering term dependence on temperature

The complete non-linear expression of the electron-phonon scattering term can be derived assuming free electrons without Umklapp collisions and a single Debye model phonon spectrum as⁵⁻⁶:

$$\Gamma_{e-ph} = \Gamma_0 \left[\frac{2}{5} + \frac{4T^5}{\theta_D^5} \int_0^{\theta_D/T} \frac{z^4}{e^z - 1} dz \right] \quad (5)$$

Where $\theta_D = 170$ K is the gold Debye temperature and $\Gamma_0 = 0.015$ eV, value that well agrees with McKay and Rayne⁷ who estimated a $\tau_0 = 1/\Gamma_0$ of ≈ 30 fs, corresponding to $\Gamma_0 \approx 0.02$ eV. We can explain this modest discrepancy through the use, in our work, of thin gold films⁸ and to a larger Debye temperature (185K) employed by McKay and Rayne in their calculations that partially offsets the increase of Γ_0 . By considering the case where $T \gg \theta_D$ we obtain $\frac{z^4}{e^z - 1} \approx z^3$, where the first order

Taylor term centred at zero is adopted. This leads to:

$$\Gamma_{e-ph} = \Gamma_0 \left[\frac{2}{5} + \frac{4T^5}{\theta_D^5} \int_0^{\theta_D/T} \frac{z^4}{e^z - 1} dz \right] \approx \Gamma_0 \left[\frac{2}{5} + \frac{4T^5}{\theta_D^5} \frac{1}{4} \frac{\theta_D^4}{T^4} \right] = \Gamma_0 \left[\frac{2}{5} + \frac{T}{\theta_D} \right] \approx \Gamma_0 \frac{T}{\theta_D} \quad (6)$$

This result clearly shows that in high temperature regime $\Gamma_{e-ph} \propto T$. Importantly, this relation is coherent with the linear dependence of metals resistivity with temperature⁹. In physical terms for $T > \theta_D$ all phonon modes are occupied and thus a linear model can be derived¹⁰⁻¹¹:

$$\Gamma_{e-ph} = \lambda \pi \frac{k_B T}{\hbar} \quad (7)$$

where λ is a metal dependent constant.

Absorption and scattering efficiency vs. damping using the complete Au dielectric function

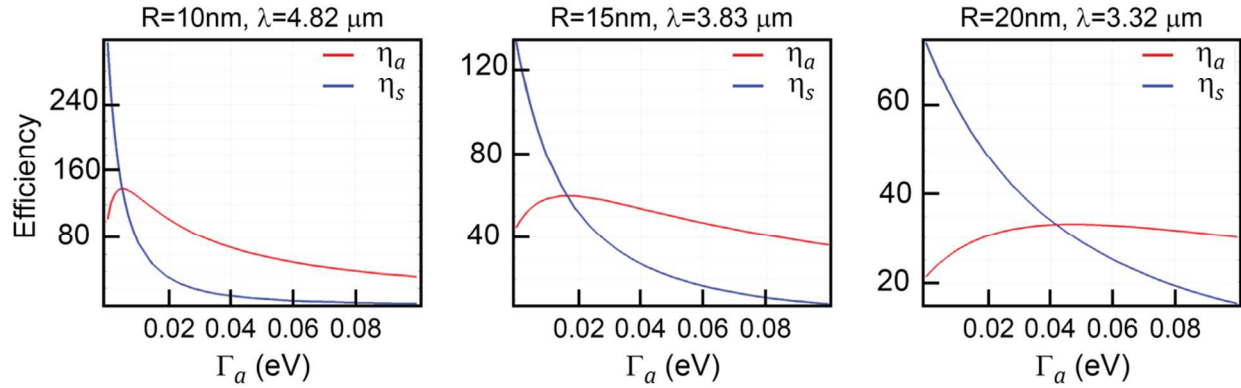


Figure S1. Absorption (red) and scattering (blue) efficiencies from numerical simulations depending on the absorption damping coefficient Γ_a for Au rods (Drude-Lorentz model) in air ($n = 1$) with height $H = 1\ \mu\text{m}$ and radius of base $R = 10, 15, 20\ \text{nm}$ respectively at their resonant wavelength: $4.35\ \mu\text{m}$, $3.52\ \mu\text{m}$ and $3.17\ \mu\text{m}$. At $\Gamma_a = 0$, absorption is given from the residual effect of interband transitions on the imaginary part of the Au dielectric function.

Dependence of absorption density on damping: H-AR and L-AR cases

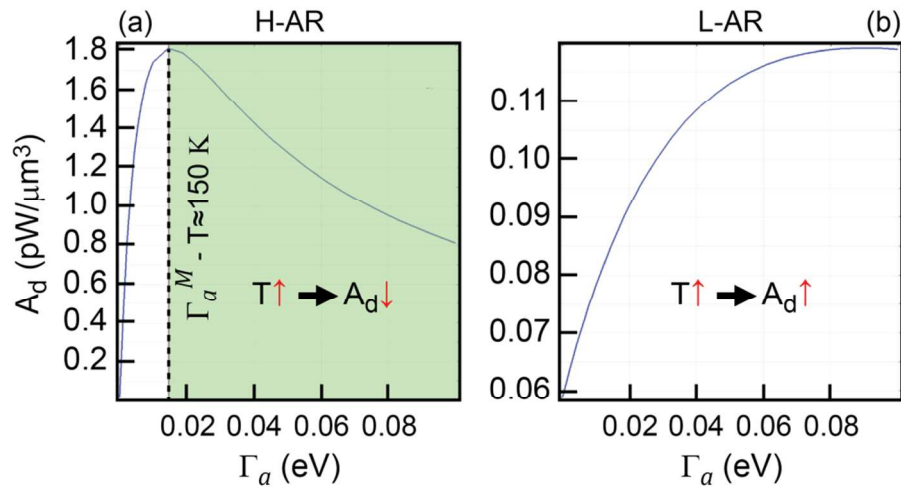


Figure S2. Absorption density as obtained from numerical simulations depending on the absorption damping coefficient Γ_a for experimental (a) H-AR and (b) L-AR antennas in air using the Drude-Lorentz model for Au permittivity. In (a) the shadow area represents the situation where an increase of temperature implies a decrease of

the absorption density. The dashed line highlights the threshold value Γ_a^M for the H-AR antenna as defined in Figure 3, corresponding to about 150 K. Vice-versa, in(b) the absorption density increases with the temperature for all considered range of Γ_a .

Dependence of field enhancement on temperature: H-AR and L-AR cases

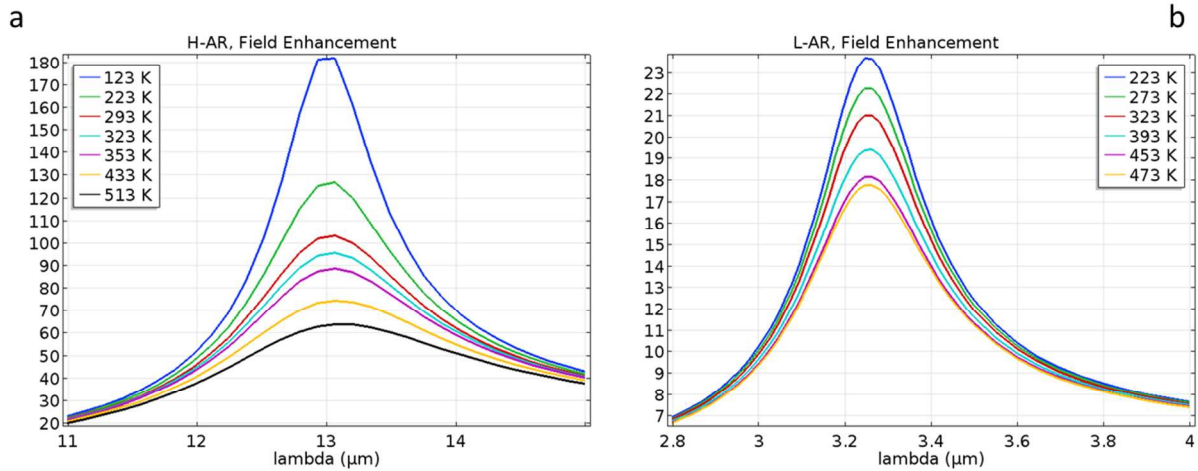


Figure S3. Field enhancement calculated at 1 nm above the edge as function of the temperature for (a) H-AR and (b) L-AR antennas. The surrounding medium is air. The temperature dependent Drude-Lorentz model for Au permittivity was employed for these calculations. A temperature (T) increase always leads to lower field enhancements as long as the imaginary part of the permittivity increases with T.

Dependence of reflectivity on temperature cycling

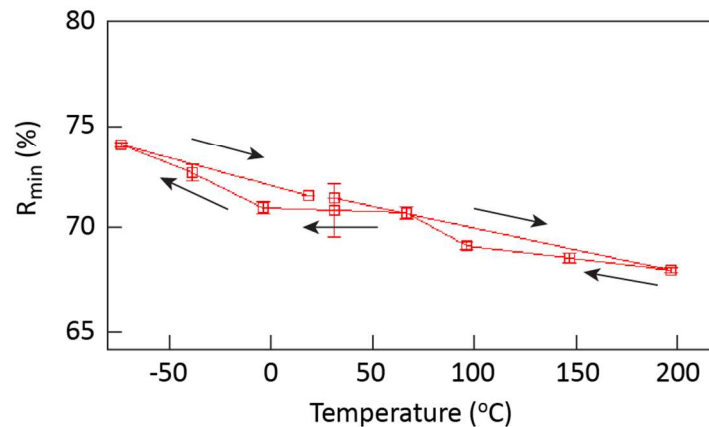


Figure S4. Example of reflectivity measurements (minimum of reflectivity) obtained by cycling the temperature starting from room temperature ($\sim 25\text{ }^{\circ}\text{C}$). The black arrows indicates how the temperature was tuned: from room temperature down to negative temperature up to $200\text{ }^{\circ}\text{C}$. Importantly, no evident change in the reflectivity was found. In this example a low aspect ratio set of antennas was employed.

Supporting Information references

- (1) Kraus, J. D.; Marhefka, R. J.; *Antennas for all applications*. McGraw-Hill, **2002**.
- (2) Staffaroni, M.; Conway, J.; Vedantam, S.; Tang, J.; Yablonovitch, E. Circuit analysis in metal-optics. *Photonics and Nanostructures - Fundamentals and Applications* **2012**, *10*, 166-176.
- (3) Engheta, N.; Salandrino, A.; Alù, A. Circuit Elements at Optical Frequencies: Nanoinductors, Nanocapacitors, and Nanoresistors. *Phys. Rev. Lett.* **2005**, *95*, 095504.
- (4) Huang, J. S.; Feichtner, T.; Biagioni, P.; Hecht, B. Impedance Matching and Emission Properties of Nanoantennas in an Optical Nanocircuit. *Nano Lett.* **2009**, *9*, 1897-1902.
- (5) Holstein, T. Optical and Infrared Volume Absorptivity of Metals. *Phys. Rev.* **1954**, *96*, 535-536.
- (6) Holstein T. Theory of transport phenomena in an electron-phonon gas. *Ann. Phys.* **1964**, *29*, 410-535.
- (7) McKay, J. A.; Rayne, J. A. Temperature dependence of the infrared absorptivity of the noble metals. *Phys. Rev. B* **1976**, *13*, 673-685.
- (8) Reddy, H.; Guler, U.; Kildishev, A. V.; Boltasseva, A.; Shalaev, V. M. Temperature-dependent optical properties of gold thin films. *Optical Materials Express* **2016**, *6*, 2776-2802.
- (9) Ashcroft, N. W.; Mermin, N. D. *Solid State Physics*. USA: BROOKS/COLE CENGAGE Learning, **1976**.
- (10) Konrad, A.; Wackenhut, F.; Hussels, M.; Meixner, A. J.; Brecht, M. Temperature Dependent Luminescence and Dephasing of Gold Nanorods. *J. Phys. Chem. C* **2013**, *117*, 21476-21482.
- (11) Kittel, C. *Introduction to solid state physics*. Hoboken, NJ: Wiley, **2005**.